Available online at www.sciencedirect.com
ScienceDirect
International Journal of Heat and Mass Transfer 51 (2008) 125–135
International Journal of HEAT and MASS TRANSFER
www.elsevier.com/locate/ijhmt

New prediction methods for CO_2 evaporation inside tubes: Part II—An updated general flow boiling heat transfer model based on flow patterns

Lixin Cheng [a], Gherhardt Ribatski [a,b], John R. Thome [a,*]

[a] Laboratory of Heat and Mass Transfer (LTCM), Faculty of Engineering (STI), École Polytechnique Fédérale de Lausanne (EPFL), Station 9, Lausanne CH-1015, Switzerland

[b] Department of Mechanical Engineering, Escola de Engenharia de São Carlos (EESC), University of São Paulo (USP), São Carlos, SP 13566-590, Brazil

Received 10 August 2006
Available online 4 June 2007

Abstract

Corresponding to the updated flow pattern map presented in Part I of this study, an updated general flow pattern based flow boiling heat transfer model was developed for CO_2 using the Cheng–Ribatski–Wojtan–Thome [L. Cheng, G. Ribatski, L. Wojtan, J.R. Thome, New flow boiling heat transfer model and flow pattern map for carbon dioxide evaporating inside horizontal tubes, Int. J. Heat Mass Transfer 49 (2006) 4082–4094; L. Cheng, G. Ribatski, L. Wojtan, J.R. Thome, Erratum to: "New flow boiling heat transfer model and flow pattern map for carbon dioxide evaporating inside tubes" [Heat Mass Transfer 49 (21–22) (2006) 4082–4094], Int. J. Heat Mass Transfer 50 (2007) 391] flow boiling heat transfer model as the starting basis. The flow boiling heat transfer correlation in the dryout region was updated. In addition, a new mist flow heat transfer correlation for CO_2 was developed based on the CO_2 data and a heat transfer method for bubbly flow was proposed for completeness sake. The updated general flow boiling heat transfer model for CO_2 covers all flow regimes and is applicable to a wider range of conditions for horizontal tubes: tube diameters from 0.6 to 10 mm, mass velocities from 50 to 1500 kg/m^2 s, heat fluxes from 1.8 to 46 kW/m^2 and saturation temperatures from −28 to 25 °C (reduced pressures from 0.21 to 0.87). The updated general flow boiling heat transfer model was compared to a new experimental database which contains 1124 data points (790 more than that in the previous model [Cheng et al., 2006, 2007]) in this study. Good agreement between the predicted and experimental data was found in general with 71.4% of the entire database and 83.2% of the database without the dryout and mist flow data predicted within ±30%. However, the predictions for the dryout and mist flow regions were less satisfactory due to the limited number of data points, the higher inaccuracy in such data, scatter in some data sets ranging up to 40%, significant discrepancies from one experimental study to another and the difficulties associated with predicting the inception and completion of dryout around the perimeter of the horizontal tubes.

Keywords: Model; Flow patterns; Flow boiling; Heat transfer; Macro-channel; Micro-channel; CO_2

1. Introduction

High reduced pressures and low surface tensions for CO_2 compared to conventional refrigerants have major effects on nucleate boiling heat transfer characteristics and previous experimental studies have suggested a clear dominance of nucleate boiling heat transfer even at very high mass flux [1–3]. Therefore, CO_2 has much higher heat transfer coefficients than those of conventional refrigerants at the same saturation temperature and the available heat transfer correlations generally underpredict the experimental data of CO_2. In addition, previous experimental studies have demonstrated that dryout trends occur earlier at

* Corresponding author. Tel.: +41 21 693 5981; fax: +41 21 693 5960.
E-mail addresses: lixincheng@hotmail.com (L. Cheng), ribatski@sc.usp.br (G. Ribatski), john.thome@epfl.ch (J.R. Thome).

0017-9310/$ - see front matter © 2007 Elsevier Ltd. All rights reserved.
doi:10.1016/j.ijheatmasstransfer.2007.04.001

Nomenclature

A_L	cross-sectional area occupied by liquid-phase, m^2
c_p	specific heat at constant pressure, J/kg K
D	internal tube diameter, m
G	total vapor and liquid two-phase mass flux, kg/m^2 s
h	heat transfer coefficient, W/m^2 K
k	thermal conductivity, W/m K
M	molecular weight, kg/kmol
N	number of data points
Pr	Prandtl number $[c_p\mu/k]$
p	pressure, Pa
p_r	reduced pressure $[p/p_{crit}]$
q	heat flux, W/m^2
Re_H	homogeneous Reynolds number $\{(GD_{eq}/\mu_V)[x+\rho_V/\rho_L(1-x)]\}$
Re_V	vapor phase Reynolds number $[GxD_{eq}/(\mu_V\varepsilon)]$
Re_δ	liquid film Reynolds number $[4G(1-x)\delta/(\mu_L(1-\varepsilon))]$
S	nucleate boiling suppression factor
T	temperature, °C
x	vapor quality
Y	correction factor

Greek symbols

δ	liquid film thickness, m
ε	cross-sectional vapor void fraction
μ	dynamic viscosity, N s/m^2
θ	angle of tube perimeter, rad
ρ	density, kg/m^3
σ	standard deviation, %
ξ	relative error, %
$\overline{\xi}$	average error, %
$\lvert\overline{\xi}\rvert$	mean error, %

Subscripts

cb	convective boiling
crit	critical
de	dryout completion
di	dryout inception
dry	dry
dryout	dryout region
eq	equivalent
h	hydraulic
IA	intermittent to annular flow transition
L	liquid
M	mist flow
nb	nucleate boiling
sat	saturation
strat	stratified flow
tp	two-phase flow
V	vapor
wavy	wavy flow
wet	on the wet perimeter

moderate vapor qualities in CO_2, particularly at high mass flux and high temperature conditions [1–3].

Thome and Ribatski [3] conducted an overall review of flow boiling heat transfer and two-phase flow of CO_2 in the literature and they found that not one of the available prediction methods was able to predict the experimental data of CO_2 well. Therefore, they suggested that a new flow boiling heat transfer prediction method should be developed and the flow boiling heat transfer model should include CO_2 effects on the annular to dryout and dryout to mist flow transitions in order to more accurately predict heat transfer coefficients at moderate/high vapor qualities. In response, Cheng et al. [1,2] have proposed a new flow boiling heat transfer model and flow pattern map for carbon dioxide evaporating inside horizontal tubes. The new flow boiling heat transfer model and flow pattern map were developed according to the model by Wojtan et al. [4,5], which is an updated version of the Kattan–Thome–Favrat [6–8] flow pattern map and flow boiling heat transfer model. The Cheng–Ribatski–Wojtan–Thome [1,2] flow boiling heat transfer model is a flow pattern based flow boiling heat transfer model which relates the flow patterns to the corresponding heat transfer mechanisms, thus, different from the numerous empirical models, such as the correlations of Chen [9], Shah [10], Gungor and Winterton [11], Kandlikar [12], Liu and Winterton [13], etc., which do not include flow pattern information. The Cheng–Ribatski–Wojtan–Thome [1,2] flow boiling heat transfer model is applicable to a wide range of conditions: tube diameters (equivalent diameters for non-circular channels) from 0.8 to 10 mm, mass fluxes from 80 to 570 kg/m^2 s, heat fluxes from 5 to 32 kW/m^2, saturation temperatures from −28 to 25 °C (the corresponding reduced pressures are from 0.21 to 0.87). The model reasonably predicts the database and it covers channel diameters found in most of CO_2 flow boiling applications. However, their model is limited by its parameter ranges from being applicable to some important applications, for example, the mass velocity ranges from 50 to 1500 kg/m^2 s in CO_2 automobile air conditioning systems. In addition, the heat fluxes in some applications go beyond the maximum value in the Cheng–Ribatski–Wojtan–Thome [1,2] flow boiling heat transfer model. Furthermore, the model does not extrapolate well to these conditions. In addition, the heat transfer model does not include heat transfer methods for CO_2 in mist flow (the mist flow heat transfer method of Wojtan et al. [5] for R22 and R410A is used and apparently it is not applicable to CO_2.) and bubbly flow regimes due to the lack of the experimental data in these regimes. Therefore, it is necessary to update the heat transfer model

for CO_2 to cover a wider range of conditions and these flow regimes.

In the present study, a new general flow boiling heat transfer model was developed by modifying the Cheng–Ribatski–Wojtan–Thome [1,2] flow boiling heat transfer model. By incorporating the updated new flow pattern map developed in Part I of this study, the new heat transfer model is physically related to the flow regimes of CO_2 evaporation, and thus correspondingly the new model has been extended to a wider range of conditions and to include new heat transfer methods in mist flow and bubbly flow regimes. The proposed new general flow boiling heat transfer model predicted reasonably well an extensive experimental database derived from the literature.

2. CO_2 flow boiling heat transfer database and analysis

2.1. Selection of CO_2 flow boiling heat transfer data

Thirteen independent experimental studies from different laboratories have been carefully selected to form the present database for flow boiling heat transfer of CO_2. These experimental studies comprise six studies [14–19] used in the Cheng–Ribatski–Wojtan–Thome [1,2] flow boiling heat transfer model and seven new studies [20–29]. The details of the test conditions of the database are summarized in Table 1. The channels tested include single circular channels and multi-channels with circular, triangular and rectangular cross-sections for a wide range of test conditions, using either electrical or fluid heating. The data were taken from tables where available or by digitizing the heat transfer data from graphs in these publications. All together, 1124 heat transfer data points (790 more than that in the previous model [1,2]) were obtained as shown in Table 1. Special care was taken in order to extract experimental data in the dryout and mist flow regimes since these are important regimes in the design of CO_2 evaporators. As no mist flow heat transfer method was developed for CO_2 in our previous study [1,2], an effort has been made here to propose a new heat transfer method for mist flow heat transfer to constitute a complete model covering all flow patterns here (hence, a preliminary bubbly flow method was also added here but no such experimental data are to be found).

In the present study, the physical properties of CO_2 have been obtained using the REFPROP of NIST [30]. For non-circular channels, equivalent diameters rather than hydraulic diameters were used for implementing flow pattern transition equations and heat transfer methods. Using an equivalent diameter gives the same mass flux as in the non-circular channel and thus correctly reflects the mean liquid and vapor velocities, something using a hydraulic diameter does not. The equivalent diameter is calculated with Eq. (1) in Part I. The heat flux of the original perimeter is applied to the perimeter of the equivalent channels using the perimeter ratio.

2.2. Analysis of the flow boiling heat transfer database

An extensive literature survey on flow boiling heat transfer related to macro-scale channels when $D_{eq} > 3$ mm and micro-scale channels when $D_{eq} \leqslant 3$ mm was conducted. Such a distinction between macro- and micro-scale by the threshold diameter of 3 mm is adopted due to the lack of a well-established theory, as pointed out by Cheng et al. [1,2] and Thome and Ribatski [3]. In order to develop a general flow boiling heat transfer prediction model, extensive comparisons of the data available in the literature were made. However, some of the data available have not been selected due to various reasons. By carefully analysing the experimental data, we have found that only 13 papers (four papers related to macro-scale and nine papers related to micro-scale), including the six papers used in our previous study [1,2], are useful. Therefore, a database including the experimental data from these papers for flow boiling heat transfer have been set up as the first step in this study. Experimental data in some papers were not utilized here for the following reasons: (i) the same data were in more than one paper by the same authors; (ii) some necessary information of the experimental conditions, viz. saturation temperature, vapor quality, etc. was missing; (iii) the data from some studies showed contradictory trends when confronted with other previous data sets and the authors did not explain why; (iv) the uncertainties of some data were very large; and (v) some data were only presented in correlated form and could not be extracted. Discussion of part of the database was already presented in our previous study [1,2]. Thus, below only some of the new data sets are discussed.

Results from four well documented studies [31–34] were disregarded in the present database for the following reasons. The data of Park and Hrnjak [31,32] at a mass velocity of 400 kg/m^2 s, a saturation temperature of −15 °C, a tube diameter of 6.1 mm and heat fluxes of 5, 10 and 15 kW/m^2 were excluded because in other CO_2 experimental studies dryout in flow boiling occurs at significantly lower vapor qualities (earlier) than for conventional refrigerants while the Park–Hrnjak data do not show any dryout (characterized by a sharp fall off in heat transfer), even at a vapor qualities up to 0.9. In addition, their heat transfer data are significantly different in value from comparable data for 6 mm and 10.06 mm tubes in two other earlier CO_2 studies [14,15], both aspects which were not addressed in their paper. The data of Hihara [33] at a mass velocity of 360 kg/m^2 s, a saturation temperature of 15 °C and a heat flux of 18 kW/m^2 with two different tube diameters, 4 and 6 mm, have flow boiling heat transfer coefficients of the 4 mm tube twice those of the 6 mm tube, which are not explainable within typical macro-scale trends nor is this finding addressed in their paper. The data of Gasche [34] at a mass velocity of 96 kg/m^2 s, a saturation temperature of 23.3 °C, a tube diameter of 0.8 mm and a heat flux of 1.81 kW/m^2 shows that the heat transfer coefficients change by more than two times in magnitude, a point that

Table 1
Database of flow boiling heat transfer for CO_2

Data source	Channel configuration and material	Equivalent diameter D_{eq} (mm)	Saturation temperature T_{sat} (°C)	Reduced pressure p_r	Mass flux G (kg/m^2 s)	Heat flux q (kW/m^2)	Data points	Heating method
Knudsen and Jensen [14][a]	Single circular tube, stainless steel	10.06	−28	0.21	80	8, 13	16	Heated by condensing R-22 vapor
Yun et al. [15][a]	Single circular tube, stainless steel	6	5, 10	0.54, 0.61	170, 240, 340	10, 15, 20	53	Electrical heating
Yoon et al. [16][a]	Single circular tube, stainless steel	7.53	0, 5. 10, 15, 20	0.47, 0.54, 0.61, 0.69 0.78	318	12.5, 16.4, 18.6	127	Electrical heating
Koyama et al. [17][a]	Single circular tube, stainless steel	1.8	0.26, 9.98, 10.88	0.47, 0.61, 0.62	250, 260	32.06	36	Electrical heating
Pettersen [18][a]	Multi-channel with 25 circular channels, aluminium	0.8	0, 10, 20, 25	0.47, 0.61, 0.78, 0.87	190, 280, 380, 570	5, 10, 15, 20	46	Heated by water
Yun et al. [19][a]	Multi-channels with rectangular channels, material not mentioned	1.52 (1.14)[a] 1.74 (1.53)[a] 1.81 (1.54)[a]	5	0.54	200, 300, 400	10, 15, 20	56	Electrical heating
Gao and Honda [20,21]	Single circular tube, stainless steel	3	−7, 10	0.39, 0.61	236, 390, 393, 590, 786, 1179	10, 20, 21	150	Electrical heating
Tanaka et al. [22]	Single circular tube, Stainless steel	1	15	0.69	360	9, 18, 36	119	Electrical heating
Hihara [23]	Single circular tube, stainless steel	1	15	0.69	720, 1440	9, 18, 36	150	Electrical heating
Shinmura et al. [24]	Multi-channel with circular channels, aluminum	0.6	5.83	0.55	400	10, 20	48	Heated by hot water
Zhao et al. [25,26]	Multi-channel with triangular channels, aluminum	1.15 (0.86)[a]	10	0.61	300	11	11	Electrical heating
Yun et al. [27,28]	Single circular channel	0.98, 2	5, 10	0.54, 0.61	1000, 1500	7.2, 7.3, 15.9, 16.2, 20, 26, 26.5, 30, 36, 46	224	Electrical heating
Jeong et al. [29]	Multi-channel with rectangular channels, aluminum	2.3 (2)[a]	0, 5, 10	0.47, 0.54, 0.61	450, 600, 750	4, 8, 12	88	Electrical heating

[a] The data used in the previous study [1,2] and the values in the brackets are hydraulic diameters (D_h), for circular channels, the hydraulic diameter equals to equivalent diameter.

was not discussed in his paper. As already pointed out in Part I, the two-phase pressure drop data of Wu et al. [35] seem to be incorrect, and thus their flow boiling heat transfer data have been excluded since the local saturation temperature is deduced from the pressure drop to determine the heat transfer coefficients.

Even so, after eliminating the data from the above studies for identifiable reasons, the remaining heat transfer database still contains some different behaviors at similar test conditions. Some discussion on this can be found in our previous study [1,2] and therefore none is presented in here. Consequently, the experimental data from the different independent studies still show somewhat different heat transfer trends and thus will affect the statistical accuracy of the new general flow boiling heat transfer model developed for CO_2 in the present study since no conclusive reasons for the contradicting trends could be found and it is not possible to say which study is right.

3. Updated flow boiling heat transfer model for CO_2

To develop a general flow boiling heat transfer prediction method, it is important that the method is not only numerically accurate but that it also correctly captures the trends in the data to be useful for heat exchanger optimization. Most importantly, the flow boiling heat transfer mechanisms should be related to the corresponding flow patterns and be physically explained according to flow pattern transitions. Besides significantly extending the range of the heat transfer database here, several new modifications were implemented in the updated general flow boiling heat transfer model and will be presented below. Changes to the flow pattern map in Part I also have an effect on the heat transfer model: the new dryout inception vapor quality correlation (Eq. (20) in Part I) and a new dryout completion vapor quality correlation (Eq. (25) in Part I) are used to better segregate the data into these regimes, which have sharply different heat transfer performances. Accordingly, the flow boiling heat transfer correlation in the dryout region was updated. In addition, a new mist flow heat transfer correlation for CO_2 was developed based on the CO_2 data and a heat transfer method for bubbly flow was proposed for completeness sake. With these modifications, a new general flow boiling heat transfer model for CO_2 was developed to meet a wider range of conditions and to cover all flow regimes.

The Kattan–Thome–Favrat [6–8] general equation for the local flow boiling heat transfer coefficients h_{tp} in a horizontal tube is used as the basic flow boiling expression:

$$h_{tp} = \frac{\theta_{dry} h_V + (2\pi - \theta_{dry}) h_{wet}}{2\pi}, \quad (1)$$

where θ_{dry} is the dry angle defined in Part I (also shown in Fig. 1 in the present paper). The dry angle θ_{dry} defines the flow structures and the ratio of the tube perimeter in contact with liquid and vapor. In stratified flow, θ_{dry} equals the stratified angle θ_{strat} which is calculated with Eq. (13)

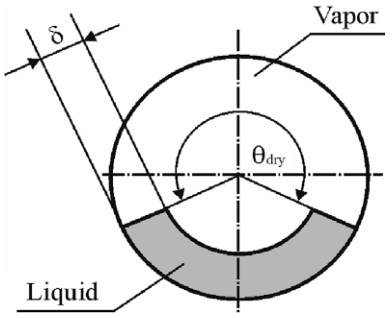

Fig. 1. Schematic diagram of film thickness.

in Part I. In annular (A), intermittent (I) and bubbly (B) flows, $\theta_{dry} = 0$. For stratified-wavy flow, θ_{dry} varies from zero up to its maximum value θ_{strat}. Stratified-wavy flow has been subdivided into three subzones (slug, slug/stratified-wavy and stratified-wavy) to determine θ_{dry}.

For slug zone (slug), the high frequency slugs maintain a continuous thin liquid layer on the upper tube perimeter. Thus, similar to the intermittent and annular flow regimes, one has

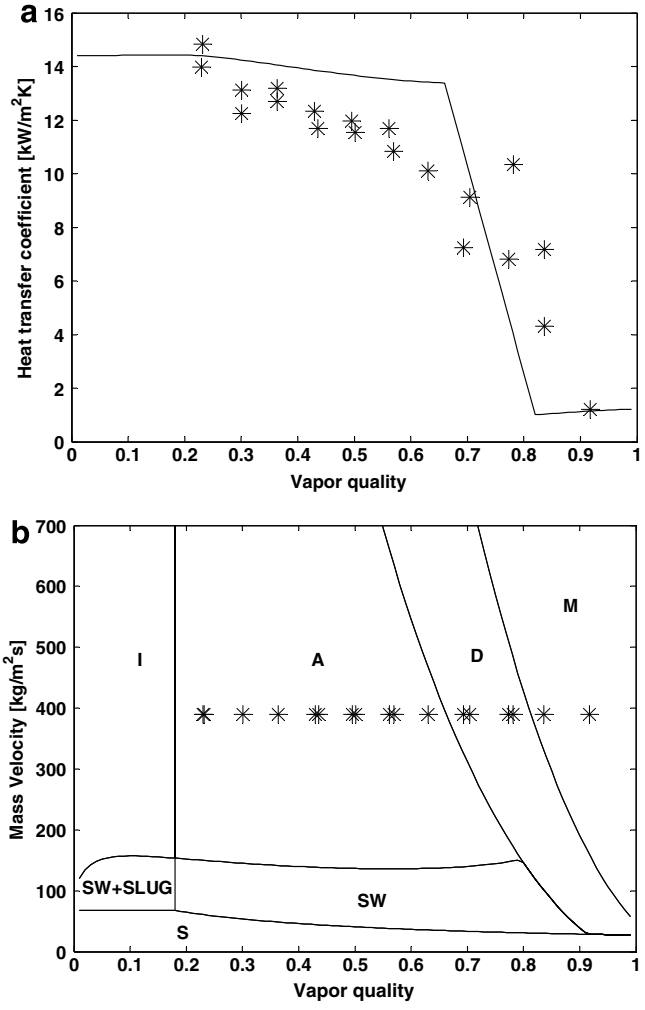

Fig. 2. (a) Comparison of the predicted heat transfer coefficients to the experimental data of Gao and Honda [20,21]; (b) the corresponding flow pattern map ($D_{eq} = 3$ mm, $G = 390$ kg/m^2 s, $T_{sat} = 10$ °C, $q = 20$ kW/m^2).

$$\theta_{dry} = 0. \quad (2)$$

For stratified-wavy zone (SW), the following equation is proposed:

$$\theta_{dry} = \theta_{strat}\left(\frac{G_{wavy} - G}{G_{wavy} - G_{strat}}\right)^{0.61}. \quad (3)$$

For slug-stratified wavy zone (Slug + SW), the following interpolation between the other two regimes is proposed for $x < x_{IA}$:

$$\theta_{dry} = \theta_{strat}\frac{x}{x_{IA}}\left(\frac{G_{wavy} - G}{G_{wavy} - G_{strat}}\right)^{0.61}. \quad (4)$$

The vapor phase heat transfer coefficient on the dry perimeter h_V is calculated with the Dittus–Boelter [36] correlation assuming tubular flow in the tube:

$$h_V = 0.023 Re_V^{0.8} Pr_V^{0.4}\frac{k_V}{D_{eq}}, \quad (5)$$

where the vapor phase Reynolds number Re_V is defined as follows:

$$Re_V = \frac{GxD_{eq}}{\mu_V \varepsilon}. \quad (6)$$

The heat transfer coefficient on the wet perimeter h_{wet} is calculated with an asymptotic model that combines the nucleate boiling and convective boiling heat transfer contributions to flow boiling heat transfer by the third power:

$$h_{wet} = \left[(Sh_{nb})^3 + h_{cb}^3\right]^{1/3}, \quad (7)$$

where h_{nb}, S and h_{cb} are respectively nucleate boiling heat transfer coefficient, nucleate boiling heat transfer suppression factor and convective boiling heat transfer coefficient and are determined in the following equations.

The nucleate boiling heat transfer coefficient h_{nb} is calculated with the Cheng–Ribatski–Wojtan–Thome [1,2] nucleate boiling correlation for CO_2 which is a modification of the Cooper [37] correlation:

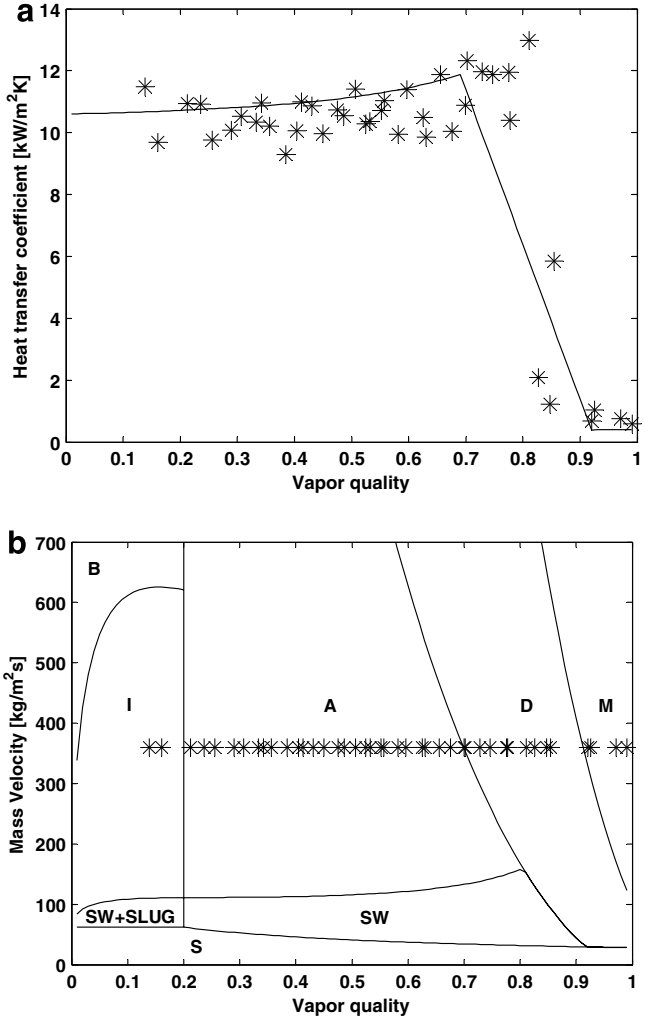

Fig. 3. (a) Comparison of the predicted flow boiling heat transfer coefficients to the experimental data of Tanaka et al. [22]; (b) the corresponding flow pattern map ($D_{eq} = 1$ mm, $G = 360$ kg/m^2 s, $T_{sat} = 15$ °C, $q = 9$ kW/m^2).

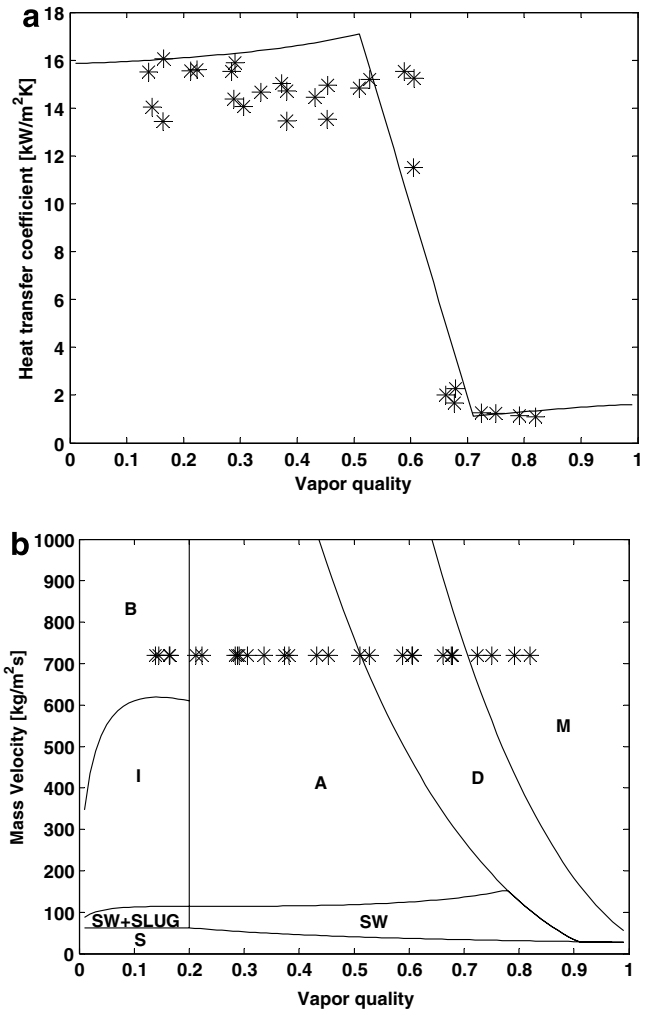

Fig. 4. (a) Comparison of the predicted heat transfer coefficients to the experimental data of Hihara [23]; (b) the corresponding flow pattern map ($D_{eq} = 1$ mm, $G = 720$ kg/m^2 s, $T_{sat} = 15$ °C, $q = 18$ kW/m^2).

$$h_{nb} = 131 p_r^{-0.0063} (-\log_{10} p_r)^{-0.55} M^{-0.5} q^{0.58}. \quad (8)$$

The Cheng–Ribatski–Wojtan–Thome [1,2] nucleate boiling heat transfer suppression factor S for CO_2 is applied to reduce the nucleate boiling heat transfer contribution due to the thinning of the annular liquid film:

$$\text{If } x < x_{IA}, \quad S = 1, \quad (9)$$

$$\text{If } x \geqslant x_{IA}, \quad S = 1 - 1.14\left(\frac{D_{eq}}{0.00753}\right)^2 \left(1 - \frac{\delta}{\delta_{IA}}\right)^{2.2}. \quad (10)$$

Furthermore, if $D_{eq} > 7.53$ mm, then set $D_{eq} = 7.53$ mm. The liquid film thickness δ shown in Fig. 1 is calculated with the expression proposed by El Hajal et al. [38]:

$$\delta = \frac{D_{eq}}{2} - \sqrt{\left(\frac{D_{eq}}{2}\right)^2 - \frac{2A_L}{2\pi - \theta_{dry}}}, \quad (11)$$

where A_L, based on the equivalent diameter, is cross-sectional area occupied by liquid-phase shown in Fig. 1 in Part I. When the liquid occupies more than one-half of the cross-section of the tube at low vapor quality, this expression would yield a value of $\delta > D_{eq}/2$, which is not geometrically realistic. Hence, whenever Eq. (11) gives $\delta > D_{eq}/2$, δ is set equal to $D_{eq}/2$ (occurs when $\varepsilon < 0.5$). The liquid film δ_{IA} is calculated with Eq. (11) at the intermittent (I) to annular flow (A) transition.

The convective boiling heat transfer coefficient h_{cb} is calculated with the following correlation assuming an annular liquid film flow from the original model [8]:

$$h_{cb} = 0.0133 Re_\delta^{0.69} Pr_L^{0.4} \frac{k_L}{\delta}, \quad (12)$$

where the liquid film Reynolds number Re_δ is defined as [7]:

$$Re_\delta = \frac{4G(1-x)\delta}{\mu_L(1-\varepsilon)}. \quad (13)$$

The void fraction ε is calculated with Eq. (8) in paper Part I and δ is calculated with Eq. (11).

The heat transfer coefficient in mist flow is calculated by a new correlation developed in this study, which is a modification of the correlation by Groeneveld [39], with a new

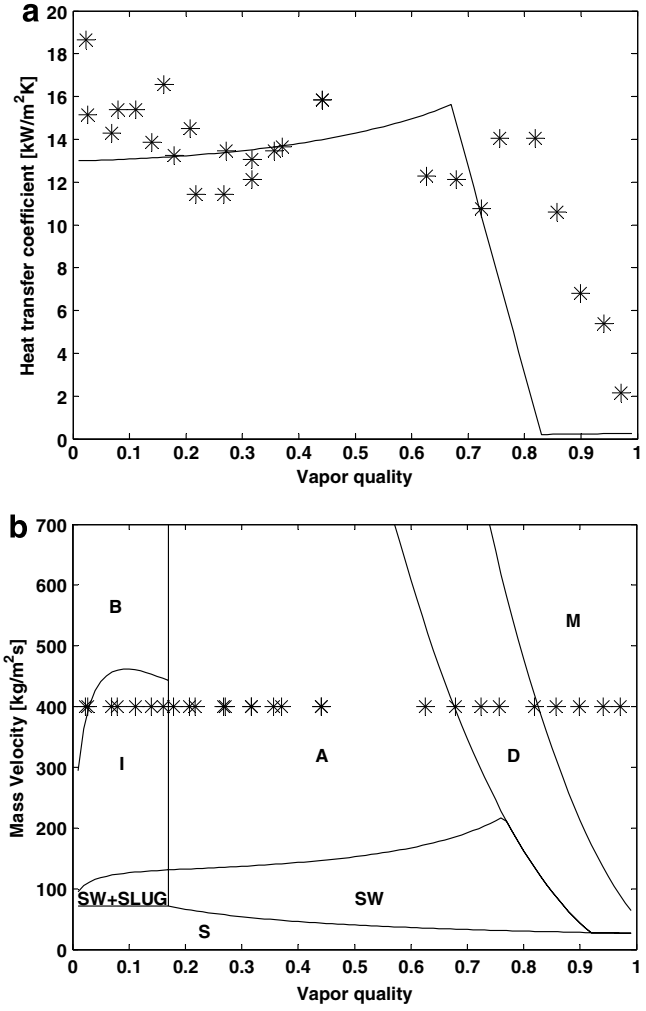

Fig. 5. (a) Comparison of the predicted heat transfer coefficients to the experimental data of Shinmura et al. [24]; (b) the corresponding flow pattern map ($D_{eq} = 0.6$ mm, $G = 400$ kg/m^2 s, $T_{sat} = 5.83$ °C, $q = 20$ kW/m^2).

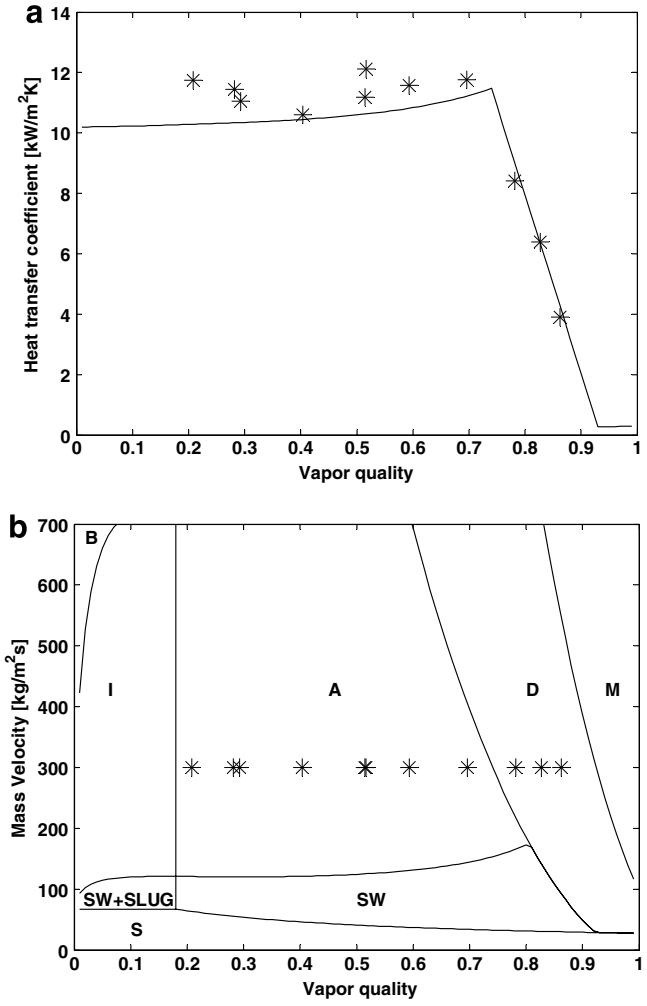

Fig. 6. (a) Comparison of the predicted heat transfer coefficients to the experimental data of Zhao et al. [25,26]; (b) the corresponding flow pattern map ($D_{eq} = 1.15$ mm, $G = 300$ kg/m^2 s, $T_{sat} = 10$ °C, $q = 11$ kW/m^2).

lead constant and a new exponent on Re_H according to CO_2 experimental data:

$$h_M = 2 \times 10^{-8} Re_H^{1.97} Pr_V^{1.06} Y^{-1.83} \frac{k_V}{D_{eq}}, \quad (14)$$

where the homogeneous Reynolds number Re_H and the correction factor Y are calculated as follows:

$$Re_H = \frac{GD_{eq}}{\mu_V}\left[x + \frac{\rho_V}{\rho_L}(1-x)\right], \quad (15)$$

$$Y = 1 - 0.1\left[\left(\frac{\rho_L}{\rho_V} - 1\right)(1-x)\right]^{0.4}. \quad (16)$$

The heat transfer coefficient in the dryout region is calculated by a linear interpolation proposed by Wojtan et al. [5]:

$$h_{dryout} = h_{tp}(x_{di}) - \frac{x - x_{di}}{x_{de} - x_{di}}\left[h_{tp}(x_{di}) - h_M(x_{de})\right], \quad (17)$$

where $h_{tp}(x_{di})$ is the two-phase heat transfer coefficient calculated with Eq. (1) at the dryout inception quality x_{di} and $h_M(x_{de})$ is the mist flow heat transfer coefficient calculated with Eq. (14) at the dryout completion quality x_{de}. Dryout inception quality x_{di} and dryout completion quality x_{de} are respectively calculated with Eqs. (20) and (25) in Part I. If x_{de} is not defined at the mass velocity being considered, it is assumed that $x_{de} = 0.999$.

A heat transfer model for bubbly flow was added to the model for completeness sake. In the absence of any data, the heat transfer coefficients in bubbly flow regime are calculated by the same method as that in the intermittent flow. Eq. (1) is used to calculate the local flow boiling heat transfer coefficients. In bubbly (B) flow, dryout angle $\theta_{dry} = 0$.

4. Comparisons of the updated general flow boiling heat transfer model to the database

The updated general flow boiling heat transfer model was compared to the database in Table 1. For comparison of other flow boiling heat transfer methods to CO_2 data, refer to [3] which showed that none of these other methods

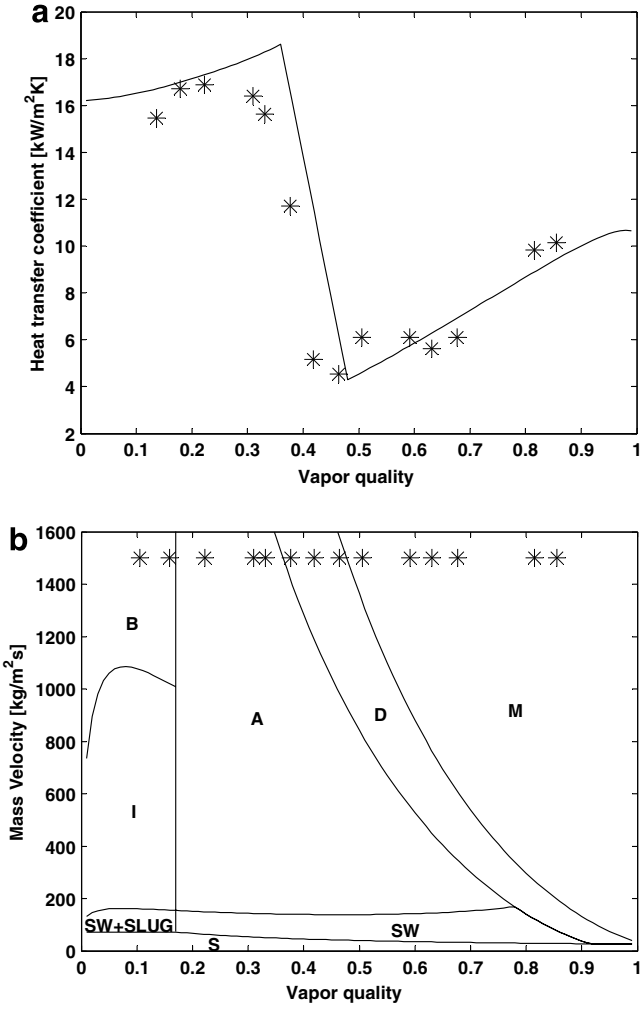

Fig. 7. (a) Comparison of the predicted heat transfer coefficients to the experimental data of Yun et al. [27,28]; (b) the corresponding flow pattern map ($D_{eq} = 2$ mm, $G = 1500$ kg/m^2 s, $T_{sat} = 5$ °C, $q = 30$ kW/m^2).

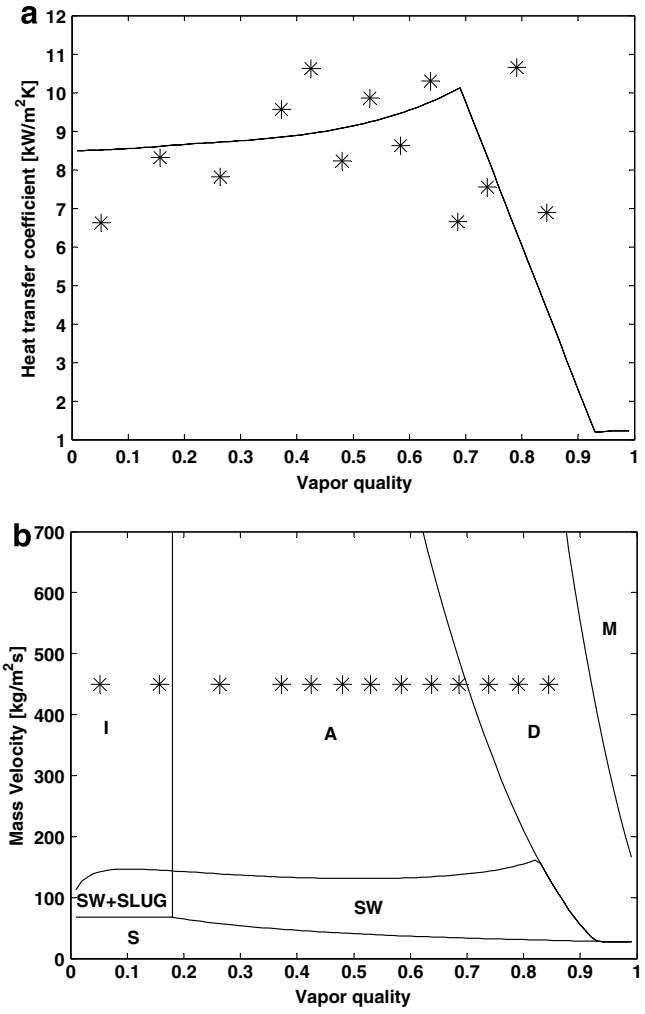

Fig. 8. (a) Comparison of the predicted heat transfer coefficients to the experimental data of Jeong et al. [29]; (b) the corresponding flow pattern map ($D_{eq} = 2.3$ mm, $G = 450$ kg/m^2 s, $T_{sat} = 10$ °C, $q = 8$ kW/m^2).

was adequate and hence that exercise is not repeated here. In fact, most studies proposed correlations based only on their own experimental data. For example, Yoon et al. [16] proposed a heat transfer correlation for CO_2 based on their experiment data for a 7.53 mm diameter tube; however, with only one macro-scale channel diameter at limited test conditions, it is not surprising that their correlation does not extrapolate well to micro-scale channels as much as one order of magnitude smaller, i.e. 0.6 mm, and this was not their intention. Furthermore, the flow pattern based flow boiling heat transfer model in [1,2] is not compared to this larger database here since (i) it does not have a mist flow heat transfer method for that part of the present database and (ii) its flow pattern map does not extrapolate to the much higher mass velocities in the new database since the dryout inception and dryout completion quality transition lines intersect at too high mass velocities and incorrectly eliminates the dryout zone at high mass velocities, which were two of the reasons to update the heat transfer model here as pointed to upon examination of this extended database.

Figs. 2–8 show the comparisons of the predicted heat transfer coefficients by the new updated general heat transfer model to selected data sets in the new flow boiling heat transfer database and the corresponding flow pattern maps. Fig. 2 shows the comparison to the data of Gao and Honda [20,21]. Fig. 3 depicts the comparison to the data of Tanaka et al. [22] while Fig. 4 presents the comparison versus the data of Hihara [23]. Fig. 5 shows the comparison to the data of Shinmura et al. [24] and Fig. 6 shows it versus the data of Zhao et al. [25,26]. Fig. 7 shows the comparison to the data of Yun et al. [27,28] and finally Fig. 8 shows the comparison to the data of Jeong et al. [29]. According to these figures, the updated general flow boiling heat transfer model not only captures the heat transfer trends well but also predicts the experimental heat transfer data well. As it is harder to predict (and harder to accurately measure) heat transfer data in the dryout and mist flow regimes, the updated general heat transfer model does not always predict the experimental data in these two flow regimes satisfactorily.

In further analysis, comparisons have also been made by classes of flows, i.e. the predictions versus all the heat transfer data excluding dryout and mist flow data (essentially the all wet perimeter data), versus all dryout heat transfer data (the partially wet perimeter data) and versus the mist flow data (all dry perimeter data). Fig. 9 shows the comparison to the first group, Fig. 10 the second and Fig. 11 the third. The statistical analysis of the predicted results is presented in Table 2, where the following fraction of the database are predicted within ±30%: 71.4% of the entire database (1124 points), 83.2% of the all wet data points (773 points), 47.6% of the partially wet data points (191 points) and 48.2% of the all dry data points (160 points).

Overall, the updated general flow boiling heat transfer model predicts the overall database quite well. However, for the dryout and mist flow regimes with partially or all

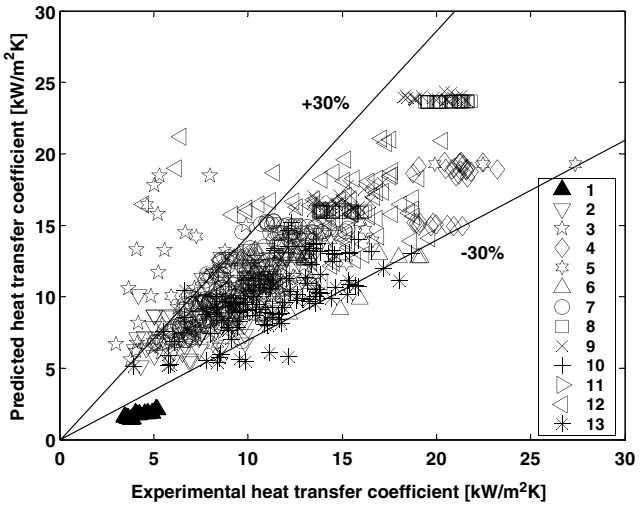

Fig. 9. Comparison of the predicted flow boiling heat transfer coefficients to all heat transfer data without the dryout and mist flow data points in the entire database: (1) Knudsen and Jensen [14], (2) Yun et al. [15], (3) Yoon et al. [16], (4) Koyama et al. [17], (5) Pettersen [18], (6) Yun et al. [19], (7) Gao and Honda [20,21], (8) Tanaka et al. [22], (9) Hihara [23], (10) Shinmura et al. [24], (11) Zhao et al. [25,26], (12) Yun et al. [27,28] and (13) Jeong et al. [29] (Note: 1–6 were used in our previous study [1,2]).

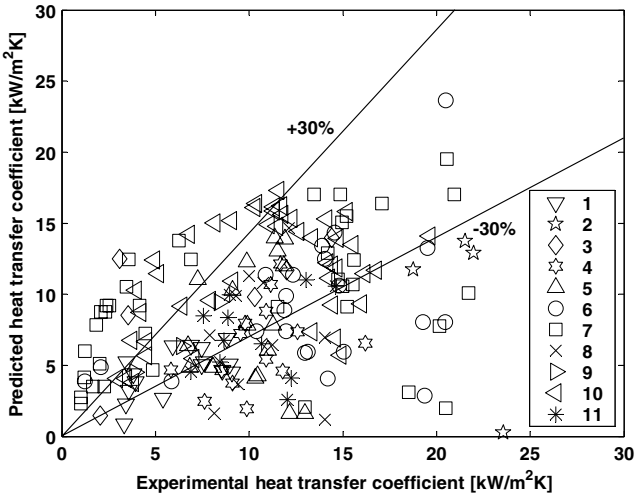

Fig. 10. Comparison of the predicted flow boiling heat transfer coefficients to all dryout heat transfer data points in the entire database: (1) Yun et al. [15], (2) Koyama et al. [17], (3) Pettersen [18], (4) Yun et al. [19], (5) Gao and Honda [20,21], (6) Tanaka et al. [22], (7) Hihara [23], (8) Shinmura et al. [24], (9) Zhao et al. [25,26], (10) Yun et al. [27,28] and (11) Jeong et al. [29] (Note: 1–4 were used in our previous study [1,2]).

dry perimeters, the heat transfer model is only partially satisfactory. For these last two regimes, many of the experimental data sets have a level of scatter ranging up 40% themselves. In part the larger errors are due to the very sharp change in trend in these data with vapor quality (see for instance Figs. 3–7a), where an error of a 2–3% in x in the energy balance of the experiments or in the prediction of x_{di} and/or x_{de} immediately results in a heat transfer prediction error of 50%. Figs. 6 and 7a happen to capture the results very well since x_{di} and/or x_{de} were predicted

Table 2
Statistical analysis of the predicted flow boiling heat transfer coefficients

Data used for comparison	Data points	Percentage of predicted points within ±30%	Mean error $\lvert\bar{\xi}\rvert$ (%)	Standard deviation σ (%)
All data points [14–29]	1124	71.4	34	68.8
All data points without the dryout and mist flow data [14–29]	773	83.2	20.9	35.6
All dryout data points [15,17–29]	191	47.6	55.4	84.8
All mist flow data points [15,17, 19–24,27–29]	160	48.2	68.7	127.8

$$\sigma = \sqrt{\frac{1}{N}\sum_{i=1}^{N}\left(\xi_i - \bar{\xi}\right)^2}; \quad \lvert\bar{\xi}\rvert = \frac{1}{N}\sum_{i=1}^{N}\lvert\xi_i\rvert; \quad \xi_i = \frac{\text{Predicted} - \text{Measured}}{\text{Measured}}.$$

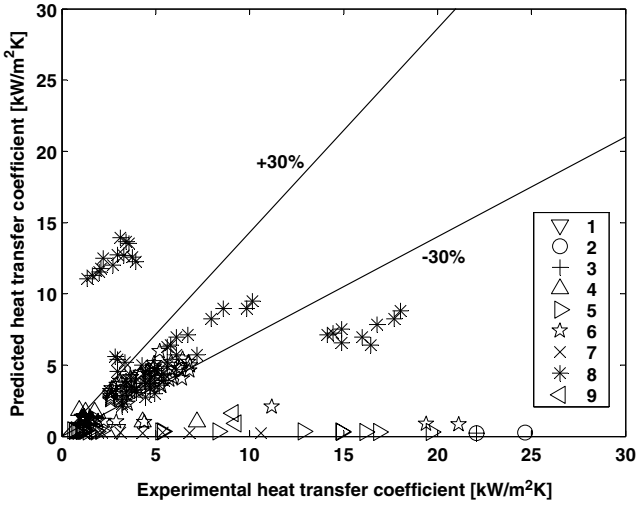

Fig. 11. Comparison of the predicted flow boiling heat transfer coefficients to all mist flow heat transfer data points in the entire database: (1) Yun et al. [15], (2) Koyama et al. [17], (3) Yun et al. [19], (4) Gao and Honda [20,21], (5) Tanaka et al. [22], (6) Hihara [23], (7) Shinmura et al. [24], (8) Yun et al. [27,28] and (9) Jeong et al. [29] (Note: 1–3 were used in our previous study [1,2]).

quite well in the flow pattern map and Figs. 10 and 11 tend to pass through the middle of the database. Therefore, more careful experiments are needed in these two regimes to provide more accurate heat transfer data, with attention to also determine the transitions x_{di} and x_{de}, in part because they are typical working conditions in the micro-scale channels of extruded multi-port aluminum tubes used for automobile air-conditioners that operate over a wide range of mass velocities up to as high as 1500 kg/m^2 s.

5. Conclusions

A general flow pattern based flow boiling heat transfer model was developed for CO_2 on the basis of the Cheng–Ribatski–Wojtan–Thome [1,2] flow boiling heat transfer model by incorporating the updated flow pattern map presented in Part I. Corresponding to the flow pattern map, the flow boiling heat transfer correlation in the dryout region was updated. In addition, a new mist flow heat transfer correlation for CO_2 was developed based on the CO_2 data and a heat transfer method for bubbly flow was proposed for completeness sake. With these modifications, the general flow boiling heat transfer model for CO_2 covers all flow regimes and is applicable to a wider range of conditions: tube diameters from 0.6 to 10 mm, mass velocities from 50 to 1500 kg/m^2 s, heat fluxes from 1.8 to 46 kW/m^2 and saturation temperatures from −28 to 25 °C (reduced pressures from 0.21 to 0.87). The general flow boiling heat transfer model was compared to an extensive experimental database (a total of 1124 data points) and good agreement between the predicted and experimental data has been found in general, where 71.4% of the entire experimental database and 83.2% of these data without the dryout and mist flow data are predicted within ±30%. However, the predicted results in the dryout and mist flow regions are not so satisfied due to the limited number of data points, their accuracy and the magnifying effect of small errors in the prediction of the transitions x_{di} and x_{de} on predicting heat transfer coefficients in these regimes.

Acknowledgements

The Laboratory of Heat and Mass Transfer (LTCM) at École Polytechnique Fédérale de Lausanne (EPFL) wishes to thank Valeo Engine Cooling in France for its financial and technical support on this CO_2 heat transfer and flow project. The constructive discussion and suggestion with Mr. Lorenzo Consolini of LTCM in the development of the CO_2 flow boiling heat transfer model are greatly appreciated.

References

[1] L. Cheng, G. Ribatski, L. Wojtan, J.R. Thome, New flow boiling heat transfer model and flow pattern map for carbon dioxide evaporating inside horizontal tubes, Int. J. Heat Mass Transfer 49 (2006) 4082–4094.

[2] L. Cheng, G. Ribatski, L. Wojtan, J.R. Thome, Erratum to: "New flow boiling heat transfer model and flow pattern map for carbon dioxide evaporating inside tubes" [Heat Mass Transfer 49 (21–22) (2006) 4082–4094], Int. J. Heat Mass Transfer 50 (2007) 391.

[3] J.R. Thome, G. Ribatski, State-of-the art of flow boiling and two-phase flow of CO_2 in macro- and micro-channels, Int. J. Refrig. 28 (2006) 1149–1168.
[4] L. Wojtan, T. Ursenbacher, J.R. Thome, Investigation of flow boiling in horizontal tubes: Part I – A new diabatic two-phase flow pattern map, Int. J. Heat Mass Transfer 48 (2005) 2955–2969.
[5] L. Wojtan, T. Ursenbacker, J.R. Thome, Investigation of flow boiling in horizontal tubes: Part II – Development of a new heat transfer model for stratified-wavy, dryout and mist flow regimes, Int. J. Heat Mass Transfer 48 (2005) 2970–2985.
[6] N. Kattan, J.R. Thome, D. Favrat, Flow boiling in horizontal tubes. Part 1: Development of a diabatic two-phase flow pattern map, J. Heat Transfer 120 (1998) 140–147.
[7] N. Kattan, J.R. Thome, D. Favrat, Flow boiling in horizontal tubes: Part 2 – New heat transfer data for five refrigerants, J. Heat Transfer 120 (1998) 148–155.
[8] N. Kattan, J.R. Thome, D. Favrat, Flow boiling in horizontal tubes: Part-3: Development of a new heat transfer model based on flow patterns, J. Heat Transfer 120 (1998) 156–165.
[9] J.C. Chen, Correlation for boiling heat transfer to saturated fluids in convective flow, Ind. Chem. Eng. Des. Dev. 5 (1966) 322–339.
[10] M.M. Shah, Chart correlation for saturated boiling heat transfer: equations and further study, ASHRAE Trans. 88 (1982) 185–196.
[11] K.E. Gungor, R.H.S. Winterton, A general correlation for flow boiling in tubes and annuli, Int. J. Heat Mass Transfer 29 (1986) 351–358.
[12] S.G. Kandlikar, A general correlation for saturated two-phase flow boiling heat transfer inside horizontal and vertical tubes, ASME J. Heat Transfer 112 (1990) 219–228.
[13] Z. Liu, R.H.S. Winterton, A general correlation for saturated and subcooled flow boiling in tubes and annuli based on a nucleate pool boiling equation, Int. J. Heat Mass Transfer 34 (1991) 2759–2766.
[14] H.J. Knudsen, R.H. Jensen, Heat transfer coefficient for boiling carbon dioxide, in: Workshop Proceedings – CO_2 Technologies in Refrigeration, Heat Pumps and Air Conditioning Systems, Trondheim, Norway, 1997, pp. 319–328.
[15] R. Yun, Y. Kim, M.S. Kim, Y. Choi, Boiling heat transfer and dryout phenomenon of CO_2 in a horizontal smooth tube, Int. J. Heat Mass Transfer 46 (2003) 2353–2361.
[16] S.H. Yoon, E.S. Cho, Y.W. Hwang, M.S. Kim, K. Min, Y. Kim, Characteristics of evaporative heat transfer and pressure drop of carbon dioxide and correlation development, Int. J. Refrig. 27 (2004) 111–119.
[17] S. Koyama, K. Kuwahara, E. Shinmura, S. Ikeda, Experimental study on flow boiling of carbon dioxide in a horizontal small diameter tube. IIR Commission B1 Meeting, Paderborn, Germany, 2001, pp. 526–533.
[18] J. Pettersen, Flow vaporization of CO_2 in microchannel tubes, Exp. Therm. Fluid Sci. 28 (2004) 111–121.
[19] R. Yun, Y. Kim, M.S. Kim, Convective boiling heat transfer characteristics of CO_2 in microchannels, Int. J. Heat Mass Transfer 48 (2005) 235–242.
[20] L. Gao, T. Honda, Effects of lubricant oil on boiling heat transfer of CO_2 inside a horizontal smooth tube, in: 42nd National Heat Transfer Symposium of Japan, 2005, pp. 269–270.
[21] L. Gao, T. Honda, An experimental study on flow boiling heat transfer of carbon dioxide and oil mixtures inside a horizontal smooth tube, in: IIR 2005 Vicenza Conference-Thermophysical Properties and Transfer Processes of Refrigerants, Vicenza, Italy, 2005, pp. 237–243.
[22] S. Tanaka, H. Daiguji, F. Takemura, E. Hihara, Boiling heat transfer of carbon dioxide in horizontal tubes, in: 38th National Heat Transfer Symposium of Japan, 2001, pp. 899–900.
[23] E. Hihara, Heat transfer characteristics of CO_2, in: Workshop Proceedings – Selected Issues on CO_2 as working Fluid in Compression Systems, Trondheim, Norway, 2000, pp. 77–84.
[24] E. Shinmura, K. Take, S. Koyama, Development of high-performance CO_2 evaporator, in: JSAE Automotive Air-Conditioning Symposium, 2006, pp. 217–227.
[25] Y. Zhao, M. Molki, M.M. Ohadi, S.V. Dessiatoun, Flow boiling of CO_2 in microchannels, ASHRAE Trans. 106 (Part I) (2000) 437–445.
[26] Y. Zhao, M. Molki, M.M. Ohadi, Heat transfer and pressure drop of CO_2 flow boiling in microchannels, in: Proceedings of the ASME Heat Transfer Division, vol. 2, 2000, pp. 243–249.
[27] R. Yun, C. Choi, Y. Kim, Convective boiling heat transfer of carbon dioxide in horizontal small diameter tubes, in: IIR/IIF-Commission B1, B2, E1 and E2-Guangzhou, China, 2002, pp. 293–303.
[28] R. Yun, Y. Kim, M.S. Kim, Flow boiling heat transfer of carbon dioxide in horizontal mini tubes, Int. J. Heat Fluid Flow 26 (2005) 801–809.
[29] S. Jeong, E. Cho, H. Kim, Evaporative heat transfer and pressure drop in a microchannel tube, in: Proceedings of the 3rd International Conference on Microchannels and Minichannels, Toronto, Ontario, Canada, Part B, 2005, pp. 103–108.
[30] REFPROP, NIST Refrigerant Properties Database 23, Gaithersburg, MD, Version 6.01, 1998.
[31] C.Y. Park, P.S. Hrnjak, Flow boiling heat transfer of CO_2 at low temperatures in a horizontal smooth tube, J. Heat Transfer 127 (2005) 1305–1312.
[32] C.Y. Park, P.S. Hrnjak, Evaporation of CO_2 in a horizontal smooth tube, in: IIR 2005 Vicenza Conference-Thermophysical Properties and Transfer Processes of Refrigerants, Vicenza, Italy, 2005, pp. 225–236.
[33] E. Hihara, Fundamental technology for carbon dioxide operated heat pumps, in: JSAE Automotive Air-Conditioning Symposium, 2006, pp. 243–262.
[34] J.L. Gasche, Carbon dioxide evaporation in a single micro-channel, J. Braz. Soc. Mech. Sci. Eng. 28 (2006) 69–83.
[35] X.M. Wu, H.Y. Zhao, W.C. Wang, L. Jing, L. Zhang, Experimental study on evaporating heat transfer of CO_2 in thin tube, J. Eng. Thermophys. 26 (2005) 823–825.
[36] F.W. Dittus, L.M.K. Boelter, Heat transfer in automobile radiator of the tubular type, Univ. Calif. Publ. Eng. 2 (1930) 443–461.
[37] M.G. Cooper, Saturation nucleate pool boiling: a simple correlation, in: 1st UK National Conference on Heat Transfer, vol. 2, pp. 785–793.
[38] J. El Hajal, J.R. Thome, A. Cavallini, Condensation in horizontal tubes, Part 2: New heat transfer model based on flow regimes, Int. J. Heat Mass Transfer 46 (2003) 3365–3387.
[39] D.C. Groeneveld, Post dry-out heat transfer at reactor operating conditions, ANS Topical Meeting on Water Reactor Safety, Salt Lake City, 1973.